Article

Thermal Conductivity of Yttria-Gadolinia Solid Solution Optical Ceramics in the Temperature Range 50–300 K

Stanislav Balabanov [1,2,*], Timofey Evstropov [1], Dmitry Permin [1,2], Olga Postnikova [1,2], Alexander Praded [3] and Pavel Popov [3]

1   G.G. Devyatykh Institute of Chemistry of High-Purity Substances of the Russian Academy of Sciences, 49 Tropinin Str., 603951 Nizhny Novgorod, Russia; evstropov@ihps-nnov.ru (T.E.); permin@ihps-nnov.ru (D.P.); postnikova@ihps-nnov.ru (O.P.)
2   Research Institute for Physics and Technology, Lobachevsky State University of Nizhny Novgorod, 23 Gagarin Ave., 603022 Nizhny Novgorod, Russia
3   Department of Physics and Mathematics, Bryansk State Academician I.G. Petrovski University, 14 Bezhitskaya Str., 341036 Bryansk, Russia; aleksandr.praded@mail.ru (A.P.); tfbgubry@mail.ru (P.P.)
*   Correspondence: balabanov@ihps-nnov.ru

Abstract: This study looked at the thermal conductivity of translucent $(Y_{1-x}Gd_x)_2O_3$ (where $0 \leq x \leq 1$) solid solution ceramics in the temperature range from 50 K to 300 K. The samples were obtained by hot pressing from high-purity nanopowders at 1600 °C, no sintering additives were used. Compositions with cubic syngony ($x \leq 0.7$) and a monoclinic one ($x \geq 0.9$) were investigated. Furthermore, a dense sample of cubic Gd_2O_3 with a LiF sintering additive was obtained and its thermal conductivity was determined ($k = 11.7$ W/(m K) at 300 K). It was shown that in the range of solid solution ceramic compositions $0.2 \leq x \leq 0.7$, the thermal conductivity was practically unchanged and close to the value $k \approx 5$ W/(m K) at 300 K.

Keywords: yttria; gadolinia; thermal conductivity; optical ceramics; solid solution

1. Introduction

Solid solutions of yttrium and gadolinium oxides are widely used in the form of optical ceramics doped with europium ions as a scintillation medium for detecting high-energy radiation, for example, in computer tomography apparatus [1]. Eu^{3+} ions have a high light output, and their emission line ($\lambda = 610$ nm) coincides with the maximum sensitivity of the most common CCDs. Gadolinium oxide, due to its high effective atomic number, has a good absorption ability of gamma- and X-ray radiation, and as a matrix component provides a more intense photoluminescence of Eu^{3+} ions compared to other REM oxides and an improved time response of scintillation. Yttrium oxide is introduced into the matrix primarily as a process additive. To achieve the optical transparency of ceramics, an almost complete removal of pores is required, which is achieved with free sintering in a vacuum or hydrogen atmosphere at temperatures in the order of 1800–1900 °C [2]. As the transformation of Gd_2O_3 from cubic to monoclinic modification occurs at ~1200–1250 °C [3], the introduction of 50–70% Y_2O_3 is necessary to increase the phase transition temperature and, accordingly, the possibility of sintering without cracking samples and the appearance of secondary scattering phases in ceramics. A concomitant purpose of introducing yttrium oxide into the ceramic composition is to reduce the absorption ability of the scintillator, for example, so that it is consistent with the corresponding characteristics of bone tissue.

Recently, optical ceramics of REM oxides of mixed composition are of increasing interest for the creation of active media for lasers [4–8]. Just like scintillators, they have in their composition an active ion, in the levels at which the emission transitions occur, but the composition of the matrix is selected for other reasons. The main idea in this case is the formation of a structure in which the active ions are in a different environment (with a

different strength of crystal field), which affects the level splitting. This provides a broadening of the luminescence spectrum, which, in particular, is necessary to increase the laser tuning range or to obtain pulses of ultra-short duration (in particular, femtosecond pulses).

However, as is known, solid solutions always have a thermal conductivity lower than at least one of the individual components. This is due to the disordering of the crystal lattice of solid solutions and, consequently, increased phonon scattering. In traditional scintillation applications, the radiation power density is usually negligible, and thus the thermal conductivity of the material does not affect the performance of the device. The situation is completely different in the case of laser applications of optical ceramics. Thermal-induced effects are one of the key factors limiting achievable laser power [9]. Solid solutions of yttrium and gadolinium oxides are of particular interest for radiation generation in the 2 µm region and beyond, for example, when doped with thulium or erbium ions. The high quantum defect in these ions ($\lambda_{pumping}$ ~800 nm and ~980 nm; $\lambda_{generation}$ ~1940 nm and ~2800 nm for Tm^{3+} and Er^{3+} ions, respectively [5,10]) means that more than half of the pump energy is converted into the vibrations of the crystal lattice due to nonradiative transitions. This creates a high thermal load on the element, and in order to create an effective laser in the 2–3 µm range, the issue of thermal conductivity of the active medium is a priority.

Since the main purpose of determining the thermal conductivity of $(Y_{1-x}Gd_x)_2O_3$ solid solution ceramics is their promising laser applications, thus, the main requirement for the samples for this study was their maximum density. In the present work, we used hot pressing of nanopowders, which was previously successfully used to obtain optical (including laser) ceramics of rare-earth metal oxides [11–14]. In these works, nanopowders were obtained by self-propagating high-temperature synthesis (SHS); the flame spray pyrolysis (FSP) method used in this work is essentially a development of it. The composition of the FSP precursor was the same as in SHS, but a flame was used to initiate the reaction. This avoided (or significantly reduced) the formation of relatively coarse agglomerates compared to SHS. The dissipation of reaction heat by massive (relative to the mass of the powder) flask walls in SHS leads to the extinguishing of precursor combustion in the adjacent layer. A lack of flame led to ineffective foaming of the precursor, thus, in this layer a fragile foam is not formed but rather rigid coral-like powders up to several microns in size. Such particles are inevitably the source of micron pores in ceramics. During FSP, all precursor droplets are in more homogeneous conditions, and thus despite some dispersion of the resulting powder in size, we did not find particles in the photographs from the scanning electron microscope that could be classified as rigid agglomerates. After the hot pressing of such powders and subsequent annealing in the air, the obtained ceramics were translucent, which we attribute to their almost full density.

This work gives an overview of the dependence of the thermal conductivity of Y_2O_3-Gd_2O_3 solid solutions on the composition in the temperature range from cryogenic to 300 K, which is most important for the operation of the active media of solid-state lasers.

2. Results and Discussion

The results of measurements of the thermal conductivity of solid solutions $(Y_{1-x}Gd_x)_2O_3$ in the form of plots of the temperature dependence $k(T)$ are shown in Figure 1. The numerical values of the thermal conductivity coefficient for several temperatures are shown in Table 1.

It can be seen that monotonically decreasing dependences $k(T)$ were mainly observed. The rate of change of dk/dT decreased as the temperature grew and the concentration of the solid solution moved away from the bound values of $x = 0$ and $x = 1$. This behavior is quite typical for solid solutions with isovalent ionic substitution [15]. The results obtained for Y_2O_3 ceramics ($x = 0$) are in good agreement with the high-temperature data of the authors [16,17]. In the case of another bound composition—Gd_2O_3 ($x = 1$)—the values of thermal conductivity of both cubic and monoclinic ceramics determined at room temperature were significantly higher than the corresponding values obtained by the authors [18]

for the same ceramics with a density of 85.7% (taking into account the recalculation to the density of 100%) and the two-phase structure. This is obviously due to the greater scattering of phonons in two-phase ceramics than in single-phase ones.
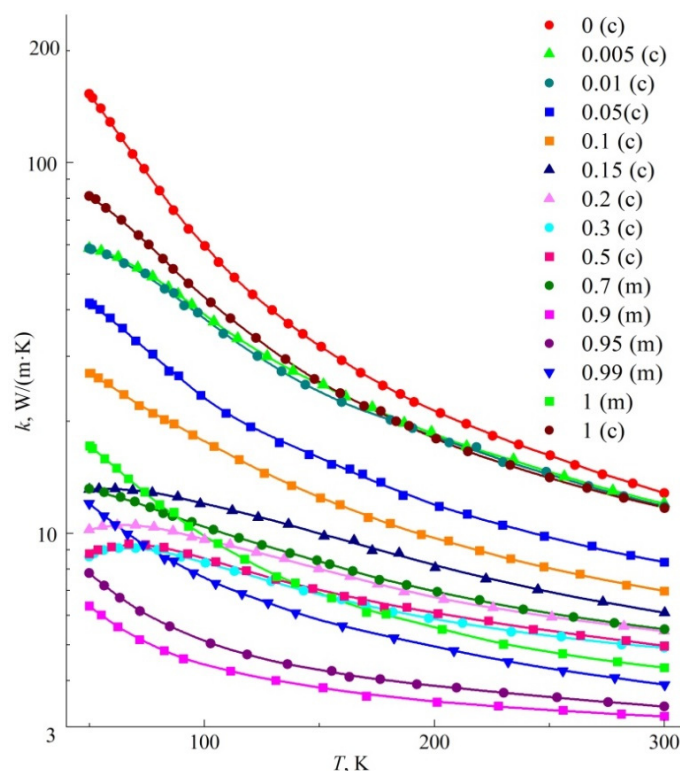

Figure 1. Temperature dependence of thermal conductivity of ceramic samples of solid solution $(Y_{1-x}Gd_x)_2O_3$. In the legend, the numbers denotes x; (c) refers to the cubic phase of the solid solution; (m) refers to the monoclinic one.

Table 1. The thermal conductivity of solid solutions $(Y_{1-x}Gd_x)_2O_3$ at different temperatures.

Gd$_2$O$_3$ Containing, mol.%	Syngony	k, W/(m K)			
		50 K	**100 K**	**200 K**	**300 K**
0	cubic	153.0	60.0	21.4	12.8
0.5	cubic	58.6	38.9	18.5	12.0
1	cubic	58.5	38.0	18.2	11.8
5	cubic	41.8	23.1	11.9	8.4
10	cubic	27.0	17.7	9.7	7.0
15	cubic	13.1	12.0	8.2	6.1
20	cubic	10.2	9.6	6.7	5.4
30	cubic	8.6	8.3	5.9	4.9
50	cubic	8.8	8.5	6.1	5.0
70	cubic	13.1	10.4	7.0	5.5
90	monoclinic	6.4	4.4	3.5	3.2
95	monoclinic	7.8	5.1	3.9	3.4
99	monoclinic	12.0	7.6	4.9	3.9
100	monoclinic	17.2	9.8	5.6	4.3
100	cubic	81.0	43.3	13.0	11.7

The k(T) curves of the samples with 15, 20, 30, and 50 mol% Gd$_2$O$_3$ differed from the others in the violation of monotonicity: as the temperatures lowered to sub nitrogen, the thermal conductivity of these samples decreased. The density of such samples also differs significantly from that calculated by the XRD method for "ideal" defect-free crystal (see Figure 2). Phonon scattering in the case of ceramic materials based on these solid

solutions mainly occurs in crystalline grains at substitutional defects due to differences in the masses and sizes of Y^{3+} and Gd^{3+} ions and at grain boundaries. The presence of pores can also be an important factor limiting the heat transfer. The magnitude of this effect can be estimated using the Maxwell–Aiken expression [19]: $k_P/k_0 = (1-P)/(1+\beta P)$, where k_P is the experimental ("effective") value of the thermal conductivity of ceramics with porosity P, determined through the ratio ρ_{rel} of real density to theoretical as $P = 1 - \rho_{rel}$, k_0 is the thermal conductivity of ceramics with zero porosity ($\rho_{rel} = 1$). The value of the parameter β depends on the shape and orientation of the pores [19] and we took it to be equal to $\frac{1}{2}$. The k_P/k_0 ratios are about 0.95 or more, which corresponds to the limits of the experimental error in determining the thermal conductivity coefficient. Given the translucency of the samples, which is usually associated with high density, we can assume that the residual pores are not a decisive factor in the studied ceramics for deviations either in thermal conductivity or in density. Thus, structural defects of another nature are formed in $(Y_{1-x}Gd_x)_2O_3$ solid solutions. In samples with a monoclinic structure ($0.9 \leq x \leq 1$), the deviation from the theoretical density was even more pronounced, probably due to the addition of stresses caused by the "frozen" phase transition.
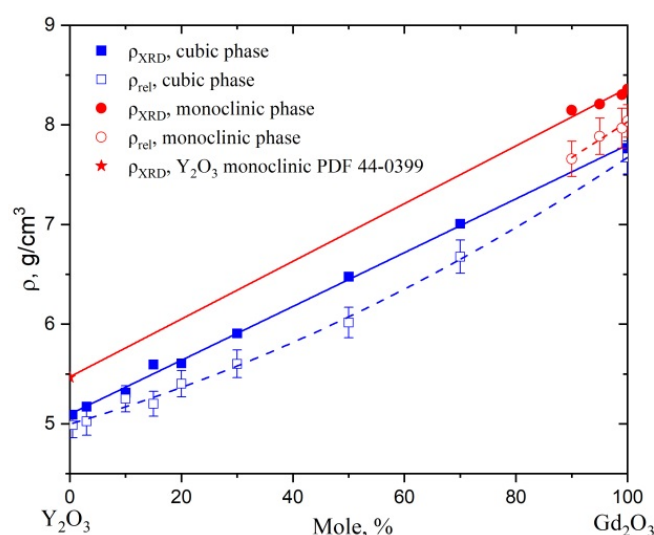

Figure 2. The experimental and theoretical XRD densities of solid solutions $(Y_{1-x}Gd_x)_2O_3$.

Figure 3 shows a plot of the concentration dependence of thermal conductivity $k(x)$ of the studied solid solution $(Y_{1-x}Gd_x)_2O_3$ at the temperature T = 300 K. The experimental points of $k(x)$ of the cubic solid solution ceramics barely deviate from the approximating curve. The concentration dependence of the specific heat resistance $w(x) = 1/k(x)$ is described satisfactorily (R^2 = 0.9924) by the polynomial of the third degree $w(x) = 3.87405 \times 10^{-7} \cdot x^3 - 1.08635 \times 10^{-4} \cdot x^2 + 7.05 \times 10^{-3} \cdot x + 8.105 \times 10^{-2}$ (x is mol.%). However, this equation has no obvious physical foundation. It can be stated that the almost flat "bottom of the pit" of the concentration dependence of the thermal conductivity $k(x)$ of $(Y_{1-x}Gd_x)_2O_3$ solid solution is at about 5 W/(m K). The minimum value of thermal conductivity in the composition with $x = 0.3$ seems to be due to the proximity to the composition with an equal volume ratio of oxides ($x \approx 0.34$).

Solid solution ceramics with monoclinic syngony ($x \geq 0.9$) have almost three times lower thermal conductivity compared to cubic ones. We did not plot the data on two-phase ceramics, which are formed in the region of compositions $0.7 < x < 0.9$ under the production modes used. As discussed above, their thermal conductivity is lower than that of single-phase ceramics, and its value depends not only on the composition, but also on the phase ratio.
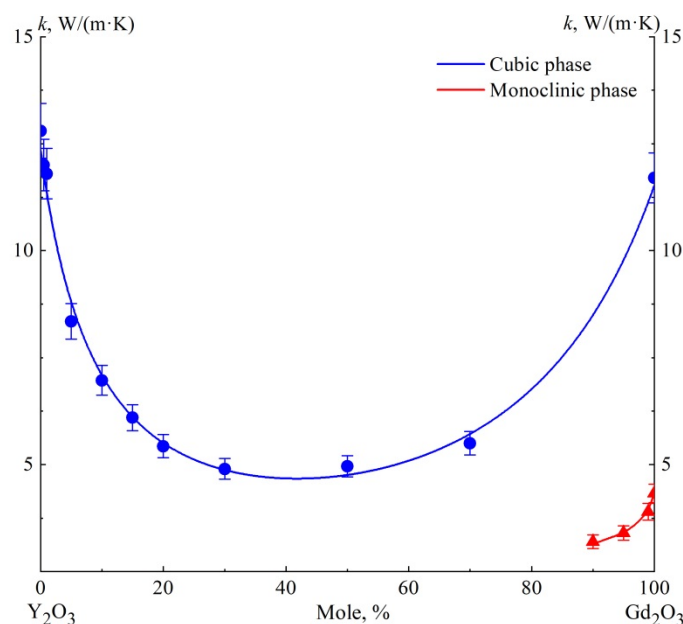
Figure 3. Dependence of thermal conductivity at 300 K of solid solution ceramics $(Y_{1-x}Gd_x)_2O_3$ on the composition.

The theoretical value of thermal conductivity for cubic Gd_2O_3 can be estimated by comparison with Y_2O_3 based on the well-known Debye expression $k = C\nu l/3$, where C is the heat capacity of the unit crystal volume, ν is the average propagation velocity of phonons (sound), and l is the phonon mean free path. From the calorimetric data [20,21] it follows that at T = 300 K the ratio $C_{Y_2O_3}/C_{Gd_2O_3}$ is a value equal to 1.055. The speed of sound is proportional to $\sqrt{E/\rho}$, where E is the Young's modulus, and ρ is the density of the material. The value of the expression $\sqrt{\rho_{Gd_2O_3}/\rho_{Y_2O_3}}$ is close to 1.23. We did not find any information about the Young's modulus value for cubic Gd_2O_3. However, the very close sizes of the lattice cells of Gd_2O_3 and Y_2O_3 allowed us to assume that the values of this elastic characteristic were also close. Therefore, the ratio $(C\nu)_{Y_2O_3}/(C\nu)_{Gd_2O_3}$ can be estimated by a value $\varepsilon = 1.055 \times 1.23 = 1.3$. Significantly larger differences in the masses of cations and anions in Gd_2O_3 with respect to Y_2O_3 also suggest a more intense phonon-phonon scattering and, accordingly, smaller values of the phonons mean a free path in Gd_2O_3. The paramagnetic properties of Gd^{3+} ions, which manifest themselves in anomalies in the thermophysical properties of gadolinia in the range of helium temperatures [22], did not significantly affect the results in the temperature range studied by us. In view of the above reasoning, the estimated value k for cubic Gd_2O_3 ceramics is $\approx$10 W/(m K) at 300 K. This is slightly less than the experimentally measured value (k = 11.7 W/(m K) at 300 K), but shows that the thermal conductivity of cubic gadolinia is near the expected value and naturally lower than that of yttria.

It is well known that for laser applications, the lutetia-based optical elements are preferable to yttria- and especially scandia-based ones at high doping levels [23]. This is related to the fact that due to differences in the atomic masses and ionic radii of the matrix and the dopant cations, the thermal conductivity of REE^{3+}:Y_2O_3 and REE^{3+}:Sc_2O_3 decreases several times compared to undoped ones, whereas in REE^{3+}:Lu_2O_3, its decrease is smoother. The experimentally measured thermal conductivity of cubic gadolinia within the measurement error was the same as the value for lutetia ceramics (12.2 W/(m K) at 300 K [24]). However, both the atomic masses and the ionic radii of common dopant ions, such as Dy^{3+}, Ho^{3+}, and especially Nd^{3+}, are noticeably closer to Gd^{3+} than to Lu^{3+}. Potentially, this means that cubic gadolinia can be used to create the most efficient laser media (such as highly doped Nd^{3+}:Gd_2O_3) in terms of reducing undesirable thermal effects. Thus, the task of developing laser-quality cubic gadolinia-based media, although challenging, is very promising.

3. Materials and Methods

3.1. Synthesis of Ceramics

The nanopowder preparation of yttria, gadolinia and their solid solution was carried out by flame spray pyrolysis (FSP) then consolidated into a dense ceramic by hot pressing. The materials used for the synthesis of precursors were yttria (99.999% Polirit, Russia), gadolinia (99.99% Polirit, Russia), nitric acid (99.9999%, Khimreaktiv, Russia) and glycine NH_2CH_2COOH (99.9%, Khimreaktiv, Russia).

First, yttrium and gadolinium nitrates were prepared by dissolving 10 g of the corresponding oxides in a stoichiometric amount of the nitric acid upon heating. A concentration of the solutions was determined by a thermogravimetric method after calcining the dry residue at 1200 °C. The nitrates were mixed in a proportion depending on the desired composition of the $(Y_{1-x}Gd_x)_2O_3$. The glycine was added to the solution of the metal nitrates in a molar ratio of 1:1. The concentration of the resulting water solution used for FSP was 0.8 mol/L.

FSP was carried out on a liquid nozzle with an internal diameter of 0.5 mm and pneumatic atomization. A propane-air mixture at a pressure of 0.3 MPa was used as a spraying gas. Metal nitrate-glycine solution was fed to the nozzle at a constant flow rate of 2 mL/min using a 3D-printed syringe pump with a stepper motor and microprocessor control. The flame temperature was maintained no higher than 800 °C (by adding excess air) to avoid sintering and agglomeration of the forming oxide nanopowders. The combustion products were mixed with air to reduce their temperature and directed to a cylindrical electrostatic precipitator (U_{spec} = 10 kV/cm), where nanopowders were collected. The yield of the finished product was about 50% by mass. Then, for complete oxidation of possible residual organic intermediates, the nanopowders were annealed in air at 900 °C for 5 h. The specific surface area of the nanopowders after annealing was about 20 g/cm^3, which approximately corresponds to the equivalent particle diameter of 40 . . . 60 nm, and was almost independent of the composition of the solid solution.

The powders were precompacted in a stainless-steel mold at a pressure of about 10 MPa. Then the compacts were isolated using a graphite paper, placed in a graphite mold (Ø20 mm) and consolidated by hot pressing in vacuum at a heating rate of 10 °C/min, a maximum temperature of 1600 °C, a holding time 1 h, and uniaxial pressure of 30 MPa using a home-made equipment. The heating was carried out by graphite heaters; the residual pressure in the chamber was about 10 Pa. Then the ceramics were calcined in air at 1000 °C for 5 h to decrease the oxygen vacancies formed in the highly reduced atmosphere of the hot press. The resulting ceramic disks were ground to rectangular parallelepipeds about 19.5 × 4.5 × 4.5 mm in size, and then polished with a diamond suspension. Cubic gadolinia was produced in a similar way, but the hot pressing temperature was 1150 °C, the holding time was 5 h, and a sintering additive of 0.1% wt. lithium fluoride was used.

3.2. Experimental

The X-ray diffraction analysis of powdered ceramics was performed on a Shimadzu LabX XRD-6000 diffractometer (Shimadzu, Japan) with Cu ($K_{\alpha1,2}$ λ = 1542 Å) radiation in the range of angles 2θ = 15–50° in 0.02° increments and 2°/min scanning speed. Qualitative and quantitative analysis of diffractograms was performed using software pack PhasanX 2.0 and UnitCell. The theoretical density of solid solutions was calculated based on the unit cell volume using the formula $\rho_{XRD} = Z \cdot M / V \cdot N_A$, where Z is the number of formula units in the unit cell (4), M is the molar mass of the solid solution, V is the unit cell volume and N_A is the Avagadro number.

The mass of the samples was measured on a laboratory analytical electronic balance KERN EW420-3NM (Kern & Sohn GmbH, Balingen, Germany) with an accuracy of ±0.5 mg. The density of the hot pressed samples was determined by the Archimedes method using weighing in distilled water. The accuracy of the density measurement was no worse than 0.1% of the theoretical density of the solid solutions.

The experimental determination of thermal conductivity in the temperature range of 50–300 K was carried out by the absolute stationary method of longitudinal heat flux. To provide a flat profile of the heating front, a heater was glued to the end surface of the sample. The temperature difference along the sample (ΔT) created by the heater did not exceed 1 K and was measured with a chromel (copper + iron) thermocouple. The values of the thermal conductivity coefficient $k(T)$ were calculated using the Fourier equation. The measurement error in determining of $k(T)$ was $\pm 5\%$. The instrumentation and measurement technique are described in detail in [25].

4. Conclusions

Nanopowders of solid solutions $(Y_{1-x}Gd_x)_2O_3$ were obtained by flame-spray pyrolysis from aqueous glycine-nitrate precursors (where $0 \leq x \leq 1$). By hot pressing at a temperature of 1600 °C for 1 h, these powders were consolidated into high density translucent ceramics. The absolute stationary method of the longitudinal heat flux method was used to measure the thermal conductivity of the obtained ceramics in the temperature range from 50 K to 300 K. The highest thermal conductivity is in neat Y_2O_3 ceramics (k = 12.8 W/(m K) at 300 K and k = 153 W/(m K) at 50 K), with an increase in the content of gadolinia, both the thermal conductivity of solid solutions and its growth as the temperature goes down significantly decrease.

In the used production modes, compositions with $0.7 < x < 0.9$ have a two-phase structure of $(Y_{1-x}Gd_x)_2O_3$ solid solution with cubic and monoclinic syngony, which leads to a significant decrease in the thermal conductivity of ceramics. The monoclinic Gd_2O_3 ceramics has a thermal conductivity of k = 4.3 W/(m K) at 300 K and k = 17.2 W/(m K) at 50 K.

Almost the same thermal conductivity of $(Y_{1-x}Gd_x)_2O_3$ solid solutions ($k \approx 5$ W/(m K) at 300 K) in the x range from 0.2 to 0.7 makes it possible not to take into account its change when optimizing the composition of optical ceramics, but to proceed from other functional or technological properties.

A dense, cubic Gd_2O_3 ceramic was made; it has high thermal conductivity both at room and cryogenic temperatures (k = 11.7 W/(m K) at 300 K and k = 81.0 W/(m K) at 50 K). The closeness of the atomic masses and ionic radii of Gd^{3+} cations and many common dopant rare-earth ions indicates that gadolinia with a cubic structure may be the most preferable laser matrix for them in terms of reducing the undesirable thermal effects.

Author Contributions: Investigation, S.B., T.E., D.P., O.P., A.P. and P.P.; writing—original draft preparation, S.B. and P.P.; writing—review and editing, S.B., T.E. and P.P. All authors have read and agreed to the published version of the manuscript.

Institutional Review Board Statement: Not applicable.

Informed Consent Statement: Not applicable.

Data Availability Statement: Not applicable.

Conflicts of Interest: The authors declare no conflict of interest.

References

1. Duclos, S.J.; Greskovich, C.D.; Lyons, R.J.; Vartuli, J.S.; Hoffman, D.M.; Riedner, R.J.; Lynch, M.J. Development of the HiLightTM scintillator for computed tomography medical imaging. *Nucl. Instrum. Methods Phys. Res. Sect. A Accel. Spectrometers Detect. Assoc. Equip.* **2003**, *505*, 68–71. [CrossRef]
2. Greskovich, C.; Duclos, S. Ceramic scintillators. *Annu. Rev. Mater. Sci.* **1997**, *27*, 69–88. [CrossRef]
3. Permin, D.A.; Boldin, M.S.; Belyaev, A.V.; Balabanov, S.S.; Koshkin, V.A.; Murashov, A.A.; Ladenkov, I.V.; Lantsev, E.A.; Smetanina, K.E.; Khamaletdinova, N.M. IR-transparent MgO-Gd_2O_3 composite ceramics produced by self-propagating high-temperature synthesis and spark plasma sintering. *J. Adv. Ceram.* **2021**, *10*, 237–246. [CrossRef]

4. Chaika, M.; Balabanov, S.; Permin, D. Spectral characteristics of "mixed" sesquioxide Yb:(Gd,Lu)$_2$O$_3$ transparent ceramics. *Opt. Mater. X* **2022**, *13*, 100123. [CrossRef]

5. Basyrova, L.; Loiko, P.; Jing, W.; Wang, Y.; Huang, H.; Dunina, E.; Kornienko, A.; Fomicheva, L.; Viana, B.; Griebner, U.; et al. Spectroscopy and efficient laser operation around 2.8 μm of Er:(Lu,Sc)$_2$O$_3$ sesquioxide ceramics. *J. Lumin.* **2021**, *240*, 118373. [CrossRef]

6. Permin, D.A.; Kurashkin, S.V.; Novikova, A.V.; Savikin, A.P.; Gavrishchuk, E.M.; Balabanov, S.S.; Khamaletdinova, N.M. Synthesis and luminescence properties of Yb-doped Y$_2$O$_3$, Sc$_2$O$_3$ and Lu$_2$O$_3$ solid solutions nanopowders. *Opt. Mater.* **2018**, *77*, 240–245. [CrossRef]

7. Basyrova, L.; Balabanov, S.; Koshkin, V.; Permin, D.; Baranov, M.; Loiko, P. Synthesis, Structure and Luminescence of Transparent «Mixed» Ceramics Dy^{3+}:(Lu,Y,La)$_2$O$_3$. In Proceedings of the 2020 International Conference Laser Optics (ICLO), St. Petersburg, Russia, 2–6 November 2020.

8. Pirri, A.; Maksimov, R.N.; Li, J.; Vannini, M.; Toci, G. Achievements and Future Perspectives of the Trivalent Thulium-Ion-Doped Mixed-Sesquioxide Ceramics for Laser Applications. *Materials* **2022**, *15*, 2084. [CrossRef] [PubMed]

9. Palashov, O.V.; Starobor, A.V.; Perevezentsev, E.A.; Snetkov, I.L.; Mironov, E.A.; Yakovlev, A.I.; Balabanov, S.S.; Permin, D.A.; Belyaev, A.V. Thermo-Optical Studies of Laser Ceramics. *Materials* **2021**, *14*, 3944. [CrossRef]

10. Antipov, O.L.; Getmanovskiy, Y.A.; Balabanov, S.S.; Larin, S.V.; Sharkov, V.V. 1940 nm, 1966 nm and 2066 nm multi-wavelength CW and passively-Q-switched operation of L-shaped Tm^{3+}:Lu$_2$O$_3$ ceramic laser in-band fiber-laser pumped at 1670 nm. *Laser Phys. Lett.* **2021**, *18*, 055001. [CrossRef]

11. Balabanov, S.; Filofeev, S.; Kaygorodov, A.; Khrustov, V.; Kuznetsov, D.; Novikova, A.; Permin, D.; Popov, P.; Ivanov, M. Hot pressing of Ho$_2$O$_3$ and Dy$_2$O$_3$ based magneto-optical ceramics. *Opt. Mater. X* **2022**, *13*, 100125. [CrossRef]

12. Balabanov, S.; Permin, D.; Evstropov, T.; Andreev, P.; Basyrova, L.; Camy, P.; Baranov, M.; Mateos, X.; Loiko, P. Hot pressing of Yb:Y$_2$O$_3$ laser ceramics with LiF sintering aid. *Opt. Mater.* **2021**, *119*, 111349. [CrossRef]

13. Balabanov, S.S.; Permin, D.A.; Rostokina, E.Y.; Palashov, O.V.; Snetkov, I.L. Characterizations of REE:Tb$_2$O$_3$ Magneto-Optical Ceramics. *Phys. Status Solidi Basic Res.* **2020**, *257*, 1900474. [CrossRef]

14. Permin, D.A.; Balabanov, S.S.; Snetkov, I.L.; Palashov, O.V.; Novikova, A.V.; Klyusik, O.N.; Ladenkov, I.V. Hot pressing of Yb:Sc$_2$O$_3$ laser ceramics with LiF sintering aid. *Opt. Mater.* **2020**, *100*, 109701. [CrossRef]

15. Berman, R.; Klemens, P.G. Thermal Conduction in Solids. *Phys. Today* **1978**, *31*, 56–57. [CrossRef]

16. Harris, D.C.; Cambrea, L.R.; Johnson, L.F.; Seaver, R.T.; Baronowski, M.; Gentilman, R.; Scott Nordahl, C.; Gattuso, T.; Silberstein, S.; Rogan, P.; et al. Properties of an Infrared-Transparent MgO:Y$_2$O$_3$ Nanocomposite. *J. Am. Ceram. Soc.* **2013**, *96*, 3828–3835. [CrossRef]

17. Liu, L.; Zhu, Q.; Zhu, Q.; Jiang, B.; Feng, M.; Zhang, L. Fabrication of fine-grained undoped Y$_2$O$_3$ transparent ceramic using nitrate pyrogenation synthesized nanopowders. *Ceram. Int.* **2019**, *45*, 5339–5345. [CrossRef]

18. Mistarihi, Q.; Sweidan, F.B.; Ryu, H.J. Thermo-physical properties of bulk Gd$_2$O$_3$ for fuel performance analysis of a lumped burnable absorber fuel design. In Proceedings of the Transactions of the Korean Nuclear Society Autumn Meeting Gyeongju, Gyeongju, Korea, 26–27 October 2017.

19. Maxwell, J. *A Treatise on Electricity and Magnetism*; Clarendon Press: Oxford, UK, 1892.

20. Goldstein, H.W.; Neilson, E.F.; Walsh, P.N. David White: The Heat Capacities Yttrium Oxide(Y$_2$O$_3$) Lanthanum Oxide (La$_2$O$_3$), and Neodymium Oxide (Nd$_2$O$_3$) from 16 to 300°K. *J. Phys. Chem.* **1959**, *63*, 1445–1449. [CrossRef]

21. Justice, B.H.; Westrum, E.F. Thermophysical properties of the lanthanide oxides. II. Heat capacities, thermodynamic properties, and some energy levels of samarium(III), gadolinium(III), and ytterbium(III) oxides from 10 to 350°K. *J. Phys. Chem.* **1963**, *67*, 345–351. [CrossRef]

22. Stewart, G.R.; Barclay, J.A.; Steyert, W.A. The specific heat of C-phase Gd$_2$O$_3$. *Solid State Commun.* **1979**, *29*, 17–19. [CrossRef]

23. Chaika, M.; Balabanov, S.; Permin, D. Optical spectra and gain properties of Er3+:Lu$_2$O$_3$ ceramics for eye-safe 1.5-μm lasers. *Opt. Mater.* **2021**, *112*, 110785. [CrossRef]

24. Peters, R.; Kränkel, C.; Petermann, K.; Huber, G. Broadly tunable high-power Yb:Lu$_2$O$_3$ thin disk laser with 80% slope efficiency. *Opt. Express* **2007**, *15*, 7075. [CrossRef] [PubMed]

25. Popov, P.A.; Sidorov, A.A.; Kul'chenkov, E.A.; Anishchenko, A.M.; Avetissov, I.C.; Sorokin, N.I.; Fedorov, P.P. Thermal conductivity and expansion of PbF2 single crystals. *Ionics* **2017**, *23*, 233–239. [CrossRef]